Dynamic Communication QoS Design for Real-Time Wireless Control Systems

Bo Chang, Guodong Zhao, Lei Zhang, Muhammad Ali Imran, Zhi Chen, and Liying Li

***Abstract*—In the coming fifth-generation (5G) cellular networks, ultra-reliable and low-latency communication (URLLC) is treated as an indispensable service to enable real-time wireless control systems. However, the extremely high quality-of-service (QoS) in URLLC causes significant wireless resource consumption. Moreover, to obtain good control performance may not always require extremely high communication QoS. In this paper, we propose a communication-control co-design scheme to reduce wireless resource consumption, where we obtain a dynamic communication QoS design method to reduce the energy consumption by jointly using extremely high QoS and a relatively low QoS. In this scheme, we first explore the control process served by different communication QoS levels and find that the whole control process can be divided into two phases, where different QoS levels have their advantages in different phases. Then, we obtain a threshold to decide when the extremely high QoS or relatively low QoS should be provided by communications. Simulation results demonstrate that our method can effectively reduce communication energy consumption while maintaining good control performance.**

***Index Terms*—URLLC; real-time wireless control; co-design; dynamic QoS allocation.**

I. Introduction

In the coming fifth-generation (5G) cellular networks, ultra-reliable and low-latency communication (URLLC) is proposed as an indispensable communication service to enable real-time wireless control systems [1]–[6]. A huge amount of applications in control systems, e.g., manufacturing, construction, and medical treatment, are expected to be supported by URLLC. For example, in health care, exoskeleton devices are strapped to human's body to enhance the moving ability. The reaction time has to be short enough to coordinate with the body, which is expected to be accomplished by real-time control.

When URLLC is used to enable real-time wireless control systems, there are some challenges to be solved, e.g., quality-of-service (QoS) requirement, communication security, spectrum allocation, network scalability, independency to the third-party infrastructure [7]. In this paper, we focus on QoS requirement in URLLC for wireless control systems. Recently, some works have been done on resource allocation for URLLC to meet the rigorous QoS, i.e., end-to-end (E2E) transmission latency and reliability, from communication perspective [8]–[14]. For example, the authors in [8] optimized the transmission power, bandwidth and antenna allocation to maximize the energy efficiency in URLLC. In [12], the authors studied the optimal number of consecutive multiple transmissions based on the allocated wireless resource for randomly emerging URLLC packet transmission. In [13], the authors analyzed the feasibility that using multiple available communication interfaces to maintain QoS requirements in URLLC. These works indicate that a huge amount of wireless resource is consumed to maintain the QoS requirements in URLLC, which significantly impedes the implementation of URLLC in real-time wireless control.

This paper intends to reduce the communication energy consumption by jointly considering communication and control sub-systems. We notice that some research on wireless control have taken communication time delay and packet loss into account [15]–[18]. In these works, the resource were scheduled by existing communication protocols, where they showed that imperfect communication coefficients have negative effect on the average control performance. However, whether worse control performance is always caused by lower communication QoS has not been discussed, which is very difficult since the allocated resource can be reduced once we find that low QoS has positive contribution on control performance in certain control stages. In [19], the authors pointed out that the resource allocation is not compromising and should be reserved to maintain the stringent QoS requirement in URLLC, which indicates that the communication QoS can be arranged during the control process.

In this paper, our motivation is to obtain a communication-control co-design scheme to reduce the usage of the extremely high QoS in URLLC, where we intend to use dynamic QoS allocation, i.e., both extremely high QoS and relatively low QoS, to serve the control process. In [20] and [21], we have shown that the hybrid high and low communication QoS can be adopted in wireless control systems. In this paper, we further discuss our dynamic QoS allocation method by communication-control co-design in details. We adopt two QoS levels to develop our method. The high level adopts the QoS in URLLC [10], and the low level adopts that required in long-term-evolution (LTE) standard [22]. The main contributions of this paper are summarized as follows.

- We analyze the relationship between communication and control, where the effects of different communication

This work was supported in part by the National Natural Science Foundation of China under Grants 61631004 and 61601094, in part by EPSRC Global Challenges Research Fund - the DARE project - EP/P028764/1, and in part by EPSRC project EP/S02476X/1. (*Corresponding author: Guodong Zhao*.)

B. Chang and Z. Chen are with the National Key Laboratory of Science and Technology on Communications, University of Electronic Science and Technology of China (UESTC), Chengdu 611731, China (e-mail: changb3212@163.com; chenzhi@uestc.edu.cn).

G. Zhao, L. Zhang, M. A. Imran, and L. Li are with the School of Engineering, University of Glasgow, Glasgow, G12 8QQ, UK (e-mail: gdngzhao@gmail.com; Lei.Zhang@glasgow.ac.uk; muhammad.imran@glasgow.ac.uk; liyingli0815@gmail.com).

Part of this work has been presented in IEEE GLOBECOM 2018 and in IEEE WF5G 2018.

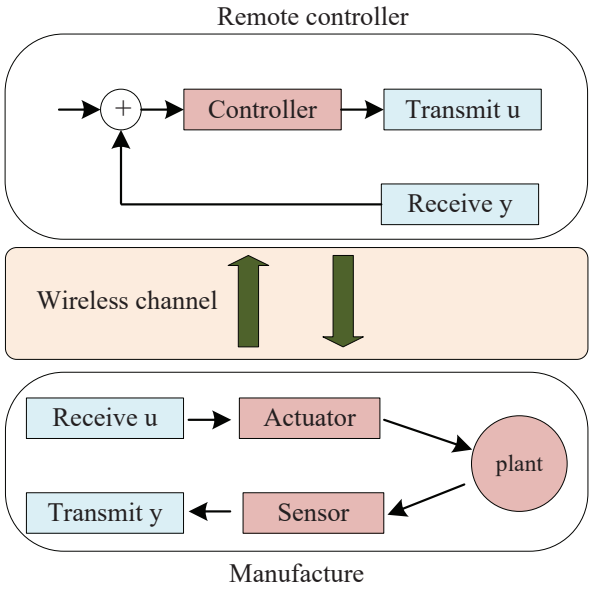

Fig. 1. A typical real-time wireless control system.

QoS on control performance are obtained. Then, we find that the control process can be divided into two phases: in the first phase, the high QoS leads to better control performance than low QoS; while in the second phase, the low QoS outperforms high QoS in terms of control performance.

- We prove that the effects of different communication QoS on control performance are different during the whole control process, where both different communication time delay and different communication reliability are discussed.
- We propose dynamic QoS selection algorithms to obtain a threshold to determine QoS allocation throughout the whole control process, which can significantly reduce the communication energy consumption while maintaining good control performance.

The rest of this paper is organized as follows. In Section II, the real-time wireless control system model with time delay and packet loss is presented. In Section III, the control process divides into two phases in terms of communication QoS. In Section IV, the dynamic communication QoS selection algorithms reducing communication energy consumption is proposed. In Section V, simulation results are provided to show the performance. Finally, Section VI concludes the paper.

II. System Model

As shown in Fig. 1, a typical real-time wireless control system is presented, where we focus on one control loop. In such a system, the uplink from the sensor to the remote controller transmits the sampling signal of the plant state y and the downlink from the remote controller to the plant transmits control input signal u. We assume that the uplink experiences transmission time delay and packet loss, while the downlink is perfect[1]. In the following of this section, we first obtain the real-time wireless control functions with communication time delay and packet loss. Then, we discuss the metrics used to evaluate the system performance from the control and communication aspects, respectively.

A. Control Function

Once the samples of the current plant state is ready at the sensor, they will be sent to the remote controller. After the calculation by the remote controller, the control input command sends back from the remote controller to the plant. Finally, the state is updated, which is determined by both the current state and the control input. According to the above process, the continuous control system is given by a linear differential equation as [23]

$$d\mathbf{x}(t) = \mathbf{A}\mathbf{x}(t)dt + \mathbf{B}\mathbf{u}(t)dt + d\mathbf{n}(t), \tag{1}$$

where $\mathbf{x}(t)$ is the plant state at time t, $\mathbf{u}(t)$ is the control input, and $\mathbf{n}(t)$ is the process disturbance caused by additive white gaussian noise (AWGN) with zero mean and variance $\mathbf{R}_n$. In addition, $\mathbf{A}$ and $\mathbf{B}$ represent the control system parameter matrices, where the elements of them are related with system physical intrinsic coefficients. The elements in system parameter matrices $\mathbf{A}$ and $\mathbf{B}$ have real physical meanings, where the details can be obtained in [24] and [25].

To obtain the discrete time control system, we assume that h_k represents the time varying sample period at the sensor, where h_k consists of the wireless transmission time delay d_k and a constant idle period $\bar{d}$. Their relationship[2] can be expressed as

$$h_k = \bar{d} + d_k, \tag{2}$$

where the sample period h_k is affected by the latency d_k. Here, $k = 1, 2, 3, \cdots, N$ represents the time index of the time sequential control process. Then, the discrete time control model with time delay d_k can be obtained as

$$\mathbf{x}_{k+1} = \mathbf{\Omega}_k \mathbf{x}_k + \mathbf{\Phi}_0^k u_k + \mathbf{\Phi}_1^k u_{k-1} + \mathbf{n}_k, \tag{3}$$

with observations at the sensor

$$\mathbf{y}_k = \mathbf{C}\mathbf{x}_k + \mathbf{n}'_k, \tag{4}$$

where $\mathbf{\Omega}_k = e^{\mathbf{A}h_k}$, $\mathbf{\Phi}_0^k = \left(\int_0^{\bar{d}} e^{\mathbf{A}t}dt\right)\mathbf{B}$, $\mathbf{\Phi}_1^k = \left(\int_{\bar{d}}^{h_k} e^{\mathbf{A}t}dt\right)\mathbf{B}$, $\mathbf{n}'_k \in \mathbb{R}^n$ is the disturbance caused by AWGN with zero mean and variance $\mathbf{R}'_n$, and k $(k = 0, 1, 2, \cdots, N)$ is the index of the sample time in the control process.

Considering the packet loss, we represent the packet loss probability as ε. Then, the successful transmission probability at time index k can be expressed as $\Pr\{l_k = 1\} = 1 - \varepsilon$. Thus, the samples received at the remote controller can be expressed as

$$\hat{\mathbf{y}}_k = \begin{cases} \mathbf{C}\mathbf{x}_k + \mathbf{n}'_k, & l_k = 1, \\ \mathbf{0}, & l_k = 0. \end{cases} \tag{5}$$

[1]The scenario that both uplink and downlink experience imperfect channel is considered as a future work.

[2]In this paper, we consider the case that the cycle time of the control loop is flexible. Thus, the proposed method is not suitable for the case where the data is sampled and transmitted in fixed period [26].

Assuming $\xi_k = (\mathbf{x}_k^T \quad u_{k-1})^T$ is the generalized state, then the control function in (3) and (4) can be rewritten as

$$\xi_{k+1} = \mathbf{\Omega}_d \xi_k + \mathbf{\Phi}_d u_k + \bar{\mathbf{n}}_k, \tag{6}$$

and

$$\hat{\mathbf{y}}'_k = l_k(\mathbf{C}_d \xi_k + \bar{\mathbf{n}}'_k), \tag{7}$$

where $\bar{\mathbf{n}}_k = (\mathbf{n}_k^T \quad 0)$, $\bar{\mathbf{n}}'_k = (\mathbf{n}_k'^T \quad 0)$, $\mathbf{\Phi}_d = \begin{pmatrix} \mathbf{\Phi}_0 \\ \mathbf{I} \end{pmatrix}$, and $\mathbf{C}_d = (\mathbf{C} \quad 0)$. According to [15], we assume $\mathbf{\Omega}_k = \mathbf{\Omega}$. Then, we have $\mathbf{\Omega}_d = \begin{pmatrix} \mathbf{\Omega} & \mathbf{\Phi}_1 \\ 0 & 0 \end{pmatrix}$. Note that the stability of the control system with transmission time delay and packet loss has be discussed in [15] and [27]. Thus, we only focus on the control performance in this paper.

B. Performance Evaluation Criterion

1) Control Performance: Control cost is usually treated as the criterion to evaluate control performance [27][28]. In this paper, the quadratic control cost is adopted, which is defined as a sum of the deviations of the state from its desired setpoint and the magnitude of the control input [15],

$$J_N = \mathbb{E}\left[\xi_N^T \mathbf{W} \xi_N + \sum_{k=0}^{N-1} \left(\xi_k^T \mathbf{W} \xi_k + u_k^T \mathbf{U} u_k\right)\right], \tag{8}$$

where $\mathbf{W}$ is the weight of the state and $\mathbf{U}$ is the weight of the control input. Since the plant state possesses the top priority in real-time control for manufacture, we assume that the weight on plant state $\mathbf{W}$ is much larger than that on control input $\mathbf{U}$ in (8).

When optimal feedback control law is used, the minimum value for J_N can be expressed as [16]

$$\begin{aligned} J_N^* =& \xi_0^T \mathbf{S}_0 \xi_0 + \mathrm{Tr}(\mathbf{S}_0 \mathbf{P}_0) + \sum_{k=0}^{N-1} (\mathrm{Tr}((\mathbf{\Omega}_d^T \mathbf{S}_{k+1} \mathbf{\Omega}_d \\ &+ \mathbf{W} - \mathbf{S}_k) \mathbf{E}_{l_k}[\mathbf{P}_{k|k}]) + \mathrm{Tr}(\mathbf{S}_{k+1} \mathbf{R}_n)), \end{aligned} \tag{9}$$

where $\xi_0 = (\mathbf{x}_0^T,\ 0)^T$. The initial state $\mathbf{x}_0$ is a white Gaussian random variable with mean $\bar{\mathbf{x}}_0$ and covariance $\mathbf{P}_0$, and the initial value is $\mathbf{S}_N = \mathbf{W}$. Furthermore, according to Appendix A, we can obtain the calculation of the parameters in (8) and (9).

2) Communication Performance: In this paper, the wireless energy consumption is considered as the criterion for communication performance, where we assume that the occupied frequency bandwidth is fixed and the bandwidth providing the best channel gain is selected. In URLLC, the channel capacity with transmission time delay and packet loss is different from the traditional Shannon capacity since the packet length is finite in URLLC [31]. Thus, we introduce the criterion for wireless resource consumption in details.

According to [31], the available uplink capacity can be obtained as

$$C_{bit} \approx \frac{T_d B_d}{\ln 2} \left\{ \ln\left(1 + \frac{h_f^2 g p}{N_0 B_d}\right) - \sqrt{\frac{V}{T_d B_d}} f_Q^{-1}(\varepsilon) \right\}. \tag{10}$$

where the available uplink rate C_{bit} is the Shannon capacity eliminating the error bits that introduced by channel dispersion, and the channel dispersion V is expressed as

$$V = 1 - \frac{1}{[1 + \frac{h_f^2 g p}{N_0 B_d}]^2}. \tag{11}$$

In (10) and (11), T_d is the allocated time resource, B_d is the allocated frequency resource, p is the transmission power, $f_Q^{-1}(\cdot)$ is the inverse of the Q-function, ε is the error probability, N_0 is the single-sided noise spectral density, g is the path-loss, and h_f is the small-scale fading.

Without loss generality, we consider the following channel path-loss model [29]

$$g_{[dB]} = -128.1 - 37.6 \lg(d), \quad \text{for} \quad d \geq \delta, \tag{12}$$

where d is the distance between two nodes, and $\delta = 35$ m is the minimum distance between them. The small-scale fading h_f follows Rayleigh distribution with mean zero and variance $\sigma_h^2 = 1$. we assume that the small fading channel coherence time is larger than the uplink frame duration, i.e., we consider block fading channel [30].

Based on the above discussion, the transmission power p^* can be calculated by solving the equation (10) for given data length C_{bit}. Thereby, the energy consumption[3] throughout the control process can be expressed as

$$E_{tol} = \sum_{k=1}^{N} p_k^*, \tag{13}$$

where p_k^* is the transmission power for the k-th sample with time delay d_k and packet loss probability ε_k.

III. Communication-Control Co-design Based Control Process Partition

Our goal is to reduce the communication energy consumption by dynamic QoS design while maintaining good control performance compared with only using extremely high QoS in URLLC. To achieve this goal, it is very important to find that whether low communication QoS level outperforms high QoS during the control process. In the following of this section, we first analyze the effects of different communication QoSs on instantaneous control performance. Based on that, we conclude that the control process can be divided into two phases, and an example is illustrated to verify our analysis.

A. Effect of Different Communication QoSs on Control Performance

In this subsection, we discuss the effect of different communication QoSs i.e., communication time delay and reliability, on control performance, and we conclude the effect of time delay and reliability, respectively.

[3]Note that from (10), it can be obtained that if the transmission power is fixed, we can also obtain the the number of resource blocks (time slot multiplied by bandwidth) that is used to meet communication QoS requirement. Thus, our results actually reflect the number of resource block to be used.

1) Different Communication Delay: From (6), the time delay is modeled into the control function. Thus, the analysis on communication time delay is based on the control parameters in (6). Since the initial control input is empty, the palnt state first increases when the time index k increases. Then, the state gradually reduces to the pre-set state since the control input is executed based on the linear feedback from the remote controller. In the following, we discuss them in more details.

According to [15], the estimated state value is approximately equal to the actual state value. We replace the state by the estimated state at the remote controller for further discussion. Then, the state covariance can be expressed as

$$\begin{aligned}\mathbf{P}_{k+1} &= \mathbb{E}\left[\mathbf{x}_{k+1}\mathbf{x}_{k+1}^T\right] \approx \mathbb{E}\left[\mathbf{x}_{k+1|k+1}\mathbf{x}_{k+1|k+1}^T\right] \\ &= \mathbb{E}[\big(\mathbf{x}_{k+1|k} + \mathbf{K}_{k+1}(\mathbf{y}_{k+1} - \mathbf{C}\mathbf{x}_{k+1|k})\big) \\ &\quad \big(\mathbf{x}_{k+1|k} + \mathbf{K}_{k+1}(\mathbf{y}_{k+1} - \mathbf{C}\mathbf{x}_{k+1|k})\big)^T] \\ &= \mathbf{\Omega}\mathbf{P}_k\mathbf{\Omega}^T + \mathbf{R}_n - l_k\mathbf{\Omega}\mathbf{P}_k\mathbf{C}^T \\ &\quad (\mathbf{C}\mathbf{P}_k\mathbf{C}^T + \mathbf{R}_{n'})^{-1}\mathbf{C}\mathbf{P}_k\Omega.\end{aligned} \tag{14}$$

For convenience, we assume $\mathbf{C} = \mathbf{I}$ and consider the case[4] with $l_k = 1$. Then, (14) can be expressed as

$$\mathbf{P}_{k+1} = \mathbf{\Omega}\mathbf{P}_k\Omega^T + \mathbf{R}_n - \mathbf{\Omega}\mathbf{P}_k(\mathbf{P}_k + \mathbf{R}_{n'})^{-1}\mathbf{P}_k\mathbf{\Omega}. \tag{15}$$

Furthermore, the state amplitude is represented by the state norm $\bar{\mathbf{x}}_k = ||\mathbf{x}_k||_2$, which can be expressed as the trace of $\mathbf{P}_{k+1}$, i.e.,

$$\begin{aligned}&Tr(\mathbf{P}_{k+1}) = Tr(\mathbf{\Omega}\mathbf{P}_k\mathbf{\Omega}^T + \mathbf{R}_n - \mathbf{\Omega}\mathbf{P}_k(\mathbf{P}_k + \mathbf{R}_{n'})^{-1}\mathbf{P}_k\mathbf{\Omega}) \\ &= Tr(\mathbf{\Omega}\mathbf{P}_k\mathbf{\Omega}^T) + Tr(\mathbf{R}_n) - Tr(\mathbf{\Omega}\mathbf{P}_k(\mathbf{P}_k + \mathbf{R}_{n'})^{-1}\mathbf{P}_k\mathbf{\Omega}).\end{aligned} \tag{16}$$

Taking derivation on $\mathbf{P}_k$ in (16), we can obtain

$$\begin{aligned}d(Tr(\mathbf{P}_{k+1})) &= Tr(\mathbf{\Omega}\mathbf{\Omega}^T d\mathbf{P}_k) - Tr(\mathbf{\Omega}d\mathbf{P}_k(\mathbf{P}_k + \\ &\quad \mathbf{R}_{n'})^{-1}\mathbf{P}_k\mathbf{\Omega} + \mathbf{\Omega}\mathbf{P}_k d(\mathbf{P}_k + \mathbf{R}_{n'})^{-1} \\ &\quad \mathbf{P}_k\mathbf{\Omega} + \mathbf{\Omega}\mathbf{P}_k(\mathbf{P}_k + \mathbf{R}_{n'})^{-1}d\mathbf{P}_k\mathbf{\Omega}) \\ &= Tr(\mathbf{\Omega}\mathbf{\Omega}^T d\mathbf{P}_k) - Tr((\mathbf{P}_k + \mathbf{R}_{n'})^{-1} \\ &\quad \mathbf{P}_k\mathbf{\Omega}\mathbf{\Omega}d\mathbf{P}_k - (\mathbf{P}_k + \mathbf{R}_{n'})^{-1}\mathbf{P}_k\mathbf{\Omega}\mathbf{\Omega} \\ &\quad \mathbf{P}_k(\mathbf{P}_k + \mathbf{R}_{n'})^{-1}\mathbf{P}_k d\mathbf{P}_k \\ &\quad + \mathbf{\Omega}\mathbf{\Omega}\mathbf{P}_k(\mathbf{P}_k + \mathbf{R}_{n'})^{-1}d\mathbf{P}_k) \\ &\approx Tr(\mathbf{\Omega}\mathbf{\Omega}^T d\mathbf{P}_k) - Tr(\mathbf{\Omega}\mathbf{\Omega}d\mathbf{P}_k \\ &\quad - \mathbf{\Omega}\mathbf{\Omega}\mathbf{P}_k d\mathbf{P}_k + \mathbf{\Omega}\mathbf{\Omega}d\mathbf{P}_k) \\ &= Tr((\mathbf{\Omega}\mathbf{\Omega}^T - 2\mathbf{\Omega}\mathbf{\Omega} + \mathbf{\Omega}\mathbf{\Omega}\mathbf{P}_k)d\mathbf{P}_k),\end{aligned} \tag{17}$$

where the approximation term is based on the fact that $\mathbf{R}_{n'}$ is small and can be ignored [15], i.e., $(\mathbf{P}_k + \mathbf{R}_{n'}) \approx \mathbf{P}_k$. If the absolute value of $d(Tr(\mathbf{P}_{k+1}))$ is large, it means that the state updates rapidly and sharply. On the contrary, if the absolute value of $d(Tr(\mathbf{P}_{k+1}))$ is small, it means that the state updates slowly and smoothly. To obtain the property of the first order derivation, we need to use the second order derivation of (16), i.e.,

$$d^2(Tr(\mathbf{P}_{k+1})) = Tr(\mathbf{\Omega}\mathbf{\Omega}d\mathbf{P}_k^2). \tag{18}$$

[4]The case with $l_k = 0$ can be obtained using the same method.

We can obtain that the second order derivation in (18) is positive, which means that the first order derivation in (17) increases monotonously. Furthermore, large elements in $\mathbf{\Omega}$ implies large second order derivation in (18), which means large gradient in (17). Considering the relationship between the wireless service and $\mathbf{\Omega}$, large time delay leads to large elements in $\mathbf{\Omega}$. Thus, for the state norm, the absolute value of the first order derivation via low QoS service is larger than that via high QoS service. This means that the state of the low QoS service updates more rapidly and sharply than the high QoS service.

Based on the above discussion and considering the stable theorem in [15], under the optimal feedback control law, we conclude that:

(1) Plant state update with latency. For either high latency or low latency, the state first deviates from the pre-set state. As the development of the control process, the state returns to the pre-set state gradually.

(2) Effect of different latency. Compered with low latency, high latency leads to larger Ω, which means that the state changes more rapidly and sharply as the time index k increases in the control process. ■

2) Different Communication Reliability: In this subsection, we discuss the effect of different communication reliability on control performance. Since the control cost considered in this paper is dominated by the plant state, the Lyapunov-like function is used to analyze the effect, which is expressed as [32]

$$\Xi_k = \xi_k^T\mathbf{W}\xi_k, \tag{19}$$

The Lyapunov-like function focuses on the plant state of each time step k, where the plant state updates with rate ρ during the control process. To satisfy the rate $\rho < 1$, the following expression holds [32]

$$\mathbb{E}[\Xi_{k+1}|\xi_k] \leq \rho\Xi_k + Tr(\mathbf{W}\mathbf{R}_n'), \tag{20}$$

where $\mathbb{E}[\cdot]$ represents the expectation operator.

Jointly considering the packet loss and Lyapunov-like control function, we can obtain

$$\begin{aligned}\mathbb{E}[\Xi(\xi_{k+1})|\xi_k] &= \Pr\{l_k = 1\}\xi_k^T(\mathbf{\Omega}_d + \mathbf{\Phi}_d)^T\mathbf{W}(\mathbf{\Omega}_d + \mathbf{\Phi}_d)\xi_k \\ &\quad + \Pr\{l_k = 0\}\xi_k^T\mathbf{\Omega}_d^T\mathbf{W}\mathbf{\Omega}_d\xi_k \\ &\quad + Tr(\mathbf{W}\mathbf{R}_n').\end{aligned} \tag{21}$$

Since $\Pr\{l_k = 0\} = 1 - \Pr\{l_k = 1\}$, we can obtain

$$\begin{aligned}&\Pr\{l_k = 1\} \geq \\ &\frac{\xi_k^T(\mathbf{\Omega}_d^T\mathbf{W}\mathbf{\Omega}_d - \rho\mathbf{W})\xi_k}{\xi_k^T(\mathbf{\Omega}_d^T\mathbf{W}\mathbf{\Omega}_d - (\mathbf{\Omega}_d + \mathbf{\Phi}_d)^T\mathbf{W}(\mathbf{\Omega}_d + \mathbf{\Phi}_d))\xi_k},\end{aligned} \tag{22}$$

which means that the upper bound of the control performance related with ρ is determined by the successful transmission probability in communication sub-systems.

Let

$$\begin{aligned}c = &\sup_{y\in\mathbb{R}^n, y\neq 0} \\ &\frac{y^T(\mathbf{\Omega}_d^T\mathbf{W}\mathbf{\Omega}_d - \rho_m\mathbf{W})y}{y^T(\mathbf{\Omega}_d^T P_m\mathbf{\Omega}_d - (\mathbf{\Omega}_d + \mathbf{\Phi}_d)^T\mathbf{W}(\mathbf{\Omega}_d + \mathbf{\Phi}_d))y}\end{aligned} \tag{23}$$

represent the supremum of the left-hand term of (22). The optimal c can be obtained by available *positive semidefinite* (PSD) programming method [33][34]. The optimal c is related with $\mathbf{\Omega}_d$, $\mathbf{\Phi}_d$, and $\Pr\{l_k = 1\}$, which means that c^* is not only determined by control parameter, but also the communication time delay and packet loss. For given transmission time delay, the relationship of the plant state update and communication reliability is related with c^*, and from (23), we can obtain the following conclusions.

(1) Plant state update with reliability. For either high reliability or low reliability, the state first deviates from the pre-set state. As the development of the control process, the state returns to the pre-set state gradually.

(2) Effect of different reliability. Compered with high reliability, low reliability leads to larger plant state update rate ρ, which means that the state changes more sharply with lower reliability. ■

B. Communication QoS Based Control Process Partition

In this subsection, based on the separate analysis on communication time delay and reliability, we conclude the effect of communication QoS on the plant state update and obtain that the control process before stable state can be divided into two phases by different communication QoSs. Then, an example is given to explain our conclusion. Finally, we discuss the communication QoS bound that should be considered when we choose the communication QoS.

1) Effect of different QoS on state update: Based on the the separate conclusions on latency and reliability, we can obtain the conclusion of the effect of different QoS on state update as following:

(1) Plant state update with communication QoS. For either high QoS or low QoS, the state first deviates from the pre-set state. As the development of the control process, the state returns to the pre-set state gradually.

(2) Effect of communication QoS. Compered with high QoS, the state changes more fast and sharply with low QoS.

Based on the above conclusion, we can obtain that compared with high QoS, the the plant state with low QoS increases faster at the initial phase, reaches to a larger state with the control process performing, and then decline faster before the state being stable. Thus, the whole control process before the state being stable can be divided into two phases based on the difference of the state changes introduced by different communication QoSs. Generally, before the state reaches to the largest value, the control process should be served by the high QoS to maintain good control performance. On the contrary, after the largest state value and before the state being stable, the control process should be served by the low QoS to reduce the communication energy consumption while maintaining good control performance, where the low communication QoS outperforms the high QoS in the control phase. Furthermore, when the state is stable, the difference between the states served by both low QoS and high QoS can be ignored. Thus, stable phase can be served by low QoS to reduce the communication energy consumption while maintaining good control performance. We conclude the above analysis in the following property.

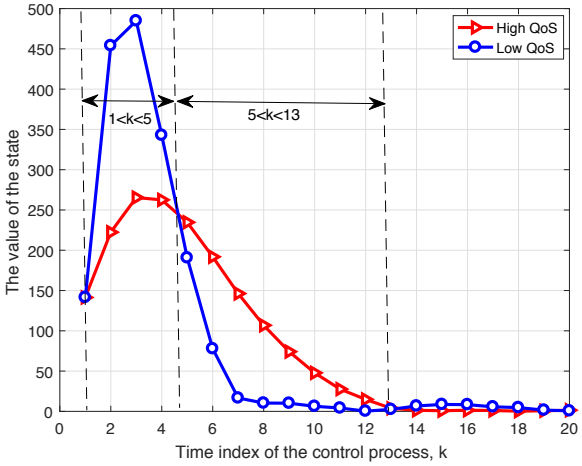

Fig. 2. An example shows the state update when the communication QoS is different.

Property 1. The whole control process can be divided into two phases in terms of communication QoS. The first phase is the control process from the initial state to the maximum state value. Then second phase is the control process from the maximum state value to the end of the control process. Furthermore, low QoS outperforms high QoS in terms of control cost and communication energy consumption when the plant state returns to the preset point from the maximum state value. ■

2) An example for the effect of different QoS: As shown in Fig. 2, an example is shown to illustrate the effect of different communication QoSs on state update in the control process, where the sampling period is 100 ms, the initial state is $(100, 100)$, and other simulation parameters are set the same as those in Section V. Here, the optimal control law is adopted, where there is no control input at the initial sampling, which would lead to that the state deviates from the pre-set state. Note that the state value is represented by the state norm $\bar{\mathbf{x}}_k = ||\mathbf{x}_k||_2$, the state value of high QoS is represented by $\bar{\mathbf{x}}_k^{high}$, and the state value of low QoS is represented by $\bar{\mathbf{x}}_k^{low}$. From the figure, we can obtain that the state update at different time index agrees with the aforementioned conclusions. On the one hand, when k increases from 1 to 13, the state value first increases and then decreases. On the other hand, from the figure, the state value with low QoS changes more sharply and rapidly than that with high QoS.

Furthermore, when $1 < k < 5$, the state value of high QoS is less than that of low value, i.e., $\bar{\mathbf{x}}_k^{high} < \bar{\mathbf{x}}_k^{low}$. Thus, from (8), we can obtain that the instantaneous control cost of high QoS is less than that of low QoS, which means that high QoS outperforms low QoS in terms of control cost when $1 < k < 5$. On the contrary, when $5 \leq k < 13$, low QoS outperforms high QoS in terms of control cost. The observation in the example shown in Fig. 2 can verify the conclusions and **Property 1** in Section III.B. Furthermore, the two control phases can be distinguished by the time index when the state served by low QoS is no more than that served by high QoS during the

control process before the state being stable.

3) Bound for Available Communication QoS: The aforementioned discussion has explained that low communication QoS outperforms compared with extreme high QoS at some stages in the control process. However, to maintain the stability of the control system, there is a bound for the low QoS, which has been discussed in [15] and we summarize it in the following lemma:

Lemma 1. The necessary and sufficient condition for stability of the adopted linear real-time wireless control system is that $|\mathbf{\Omega}_d|^2\varepsilon_{th} < \varepsilon_{th}$ and $\mathbf{\Phi}_d$ is invertible, where $|\mathbf{\Omega}_d| = \max|\lambda(\mathbf{\Omega}_d)|$ is the largest eigenvalue of the matrix $\mathbf{\Omega}_d$. ■

By choosing the QoS satisfying the conditions in Theorem 1, the proposed method can be performed while maintaining stability of the control systems.

IV. Control Process Partition Based Dynamic QoS Design

In this section, we discuss how the extremely high QoS and relatively low QoS are dynamically used in the control process. Based on the stability conditions in Section III, we can obtain that the available communication QoS is in a continuous region. Thus, the optimal dynamic QoS selection method can be obtained within this region theoretically. According to the conclusions about the effect of different QoS on state update, we can obtain that the method only considering two levels of QoS is optimal, where the one QoS level is as high as that can be provided and the other one is the lower bound to maintain the stability. Considering the compatibility with the exist and upcoming cellular networks, two communication QoSs are adopted in this paper: the first one is the QoS required in URLLC, which is the highest QoS required in the upcoming 5G; the second one is that used in current LTE cellular networks. Both of the two levels are included in the continuous region. From Property 1, there is a cross-point when the state returns to the preset state from the maximum value. In the following of this section, we discuss how to find the cross-point using a threshold to determine the dynamic communication QoS allocation by jointly considering the state update and time index k.

A. Ideal Threshold Design

In this subsection, we obtain a time index threshold k_{th} for dynamic communication QoS allocation by observing the state update with disturbance. This method is summarized in Algorithm 1. In step 1, we assume that the disturbance $\overline{\mathbf{n}}_k$ is perfectly known at the remote controller. Then, with the perfect information about the state update function in step 1 and 2, the controller can calculate the state in the next time index $k+1$. Thus, by comparing the states served by the two communication QoS levels, the time index threshold k_{th} can be obtained.

In fact, it is unrealistic to obtain k_{th} by Algorithm 1 since the perfect disturbance cannot be obtained by the controller. Thus, Algorithm 1 is an ideal threshold design (ITD) method. To obtain the threshold k_{th}, we propose a relaxed method in the next subsection.

Algorithm 1 The ITD method

Input: $\mathbf{A}$, $\mathbf{B}$, $\mathbf{C}$, d_k, ε, the initial state $\mathbf{x}_0$, $k_{th}=0$, the process disturbance $\mathbf{n}(t)$, and the AWGN of the observation $\mathbf{R}'_n$

1: According to $\xi_{k+1} = \mathbf{\Omega}_d\xi_k + \mathbf{\Phi}_d u_k + \overline{\mathbf{n}}_k$, the updated state can be calculated when high URLLC QoS is considered
2: According to $\xi'_{k+1} = \mathbf{\Omega}'_d\xi'_k + \mathbf{\Phi}'_d u'_k + \overline{\mathbf{n}}_k$, the updated state can be calculated when low QoS is considered
3: **while** $\xi_{k+1} < \xi'_{k+1}$, $(k>0)$ **do**
4: $\quad k_{th} = k_{th} + 1$
5: **end while**

Output: k_{th}

B. Relaxed Threshold Design

To obtain an effective threshold, we propose a relaxed threshold design (RTD) method, where the disturbance is ignored. Thus, the proposed RTD method can work well when the disturbance noise is small. If $\overline{\mathbf{n}}_k \ll \xi_k$, then the disturbance noise can be ignored and the plant update function in (6) can be expressed as

$$\xi_{k+1} \approx \mathbf{\Omega}_d\xi_k + \mathbf{\Phi}_d u_k. \tag{24}$$

To obtain the RTD algorithm, we further assume that the sensor at the plant can receive signals from the remote controller. Then, the control process can be virtually performed at the remote controller. The threshold k_{th} can be obtained when $\bar{\mathbf{x}}_k^{high} < \bar{\mathbf{x}}_k^{low}$ changes to $\bar{\mathbf{x}}_{k+1}^{high} > \bar{\mathbf{x}}_{k+1}^{low}$. Finally, the remote controller sends the calculation results back to the sensor to determine the dynamic QoS design, where the high URLLC QoS service is adopted when $k < k_{th}$ and the low QoS service is adopted when $k \geq k_{th}$. The process is summarized in Algorithm 2.

Algorithm 2 The proposed RTD method to determine the threshold

Input: $\mathbf{A}$, $\mathbf{B}$, $\mathbf{C}$, d_k, ε, the initial state $\mathbf{x}_0$, and $k_{th}=0$

1: According to $\xi_{k+1} = \mathbf{\Omega}_d\xi_k + \mathbf{\Phi}_d u_k$, the updated state can be calculated when high QoS is considered
2: According to $\xi'_{k+1} = \mathbf{\Omega}'_d\xi'_k + \mathbf{\Phi}'_d u'_k$, the updated state can be calculated when low QoS is considered
3: **while** $\bar{\xi}_k < \bar{\xi}'_k$, $(k>1)$ **do**
4: $\quad k_{th} = k_{th} + 1$
5: **end while**

Output: k_{th}

From the above discussion, the proposed RTD method can obtain good performance when the disturbance is small. The large disturbance case will be discussed in the simulation results. In Section V, we obtain the system performance of our proposed method.

V. Simulation Results

In this section, we provide simulation results to demonstrate the performance of the proposed method, where the system model is the same as that in Fig. 1. The maximum time delay

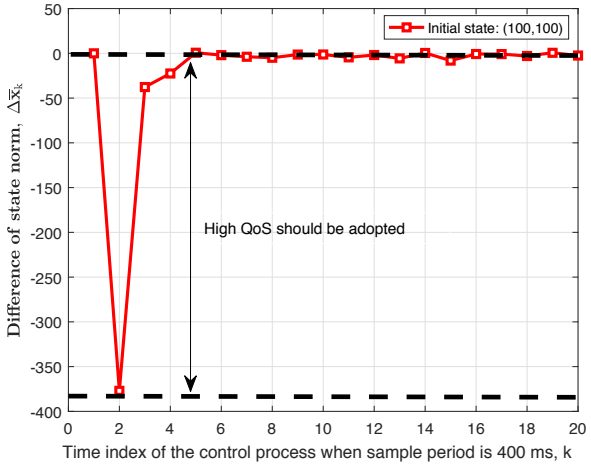

Fig. 3. The difference of the state norm with different time index when sample period is 400 ms.

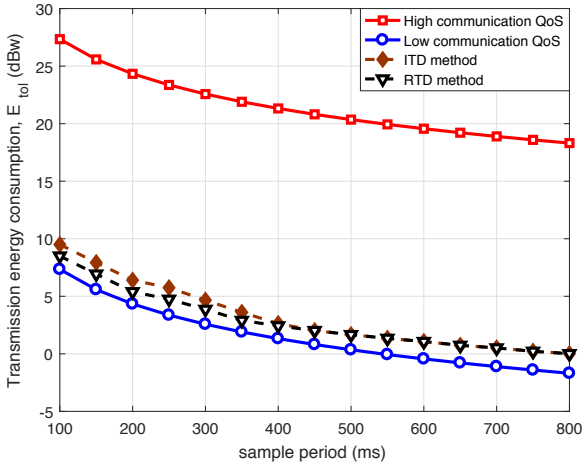

Fig. 5. Transmission energy consumption with different control sample period.

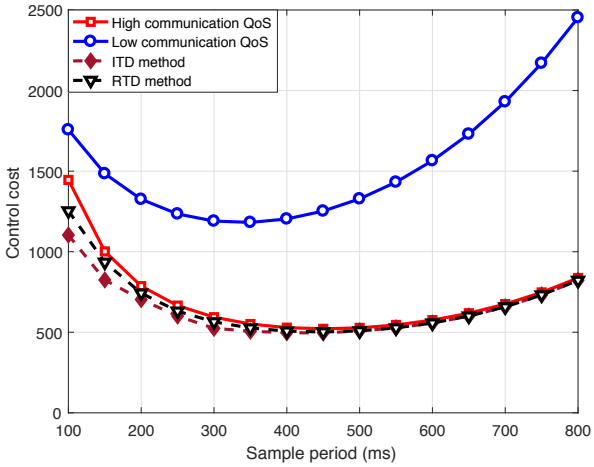

Fig. 4. Control cost with different control sample period.

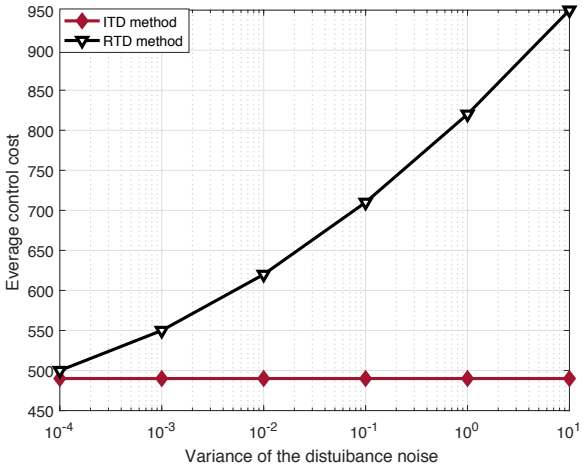

Fig. 6. Control cost with different disturbance noise.

of the high URLLC QoS is 1 ms and the maximum packet loss ε is 10^{-5} [10]. In contrast, the maximum time delay of the low QoS is 100 ms and the maximum packet loss ε is 10^{-3}. The control parameters are as follows: $\mathbf{A} = \begin{pmatrix} 2 & 14 \\ 0 & 1 \end{pmatrix}$, $\mathbf{B} = \begin{pmatrix} 0 \\ 1 \end{pmatrix}$, $\mathbf{C} = \begin{pmatrix} 1 & 0 \\ 0 & 1 \end{pmatrix}$, $\mathbf{P}_0 = 0.01\mathbf{I}$, $\mathbf{W} = \mathbf{I}$, $\mathbf{U} = 0.0001$, $\mathbf{R}_{n'} = 0.01\mathbf{I}$, and the initial state is $(100, 100)$. The length of the discrete control process is $N = 10000$. In the simulations, there are 100 bits in each packet, the communication system bandwidth is 1 MHz, the single-sided noise spectral density is -174 dBm/Hz, and the distance between the sensor and the controller is 100 m. Each curve is obtained by 10000 Monte Carlo trails if there is no extra declaration.

A. Performance with Small Disturbance Noise

In this subsection, we consider the control and communication performance when the disturbance noise is small, where $\mathbf{R}_n = 0.0001\mathbf{I}$.

1) Control Performance: Fig. 3 shows the difference of the state norm when sample period is 600 ms, where the simulation conditions are the same as that in Fig. 2. The y-axis is defined as the difference between the state norm of the control system serviced by high QoS and that serviced by low QoS, i.e., $\Delta\bar{\mathbf{x}}_k \triangleq \bar{\mathbf{x}}_k^{high} - \bar{\mathbf{x}}_k^{low}$. If $\Delta\bar{\mathbf{x}}_k < 0$, it means that high QoS leads to smaller state than low QoS at time index k, where high QoS is critical and should be adopted. Otherwise, if $\Delta\bar{\mathbf{x}}_k > 0$, low QoS can be adopted to reduce the energy consumption. Compared with the curve with initial state $(100, 100)$ when sample period is 100 ms in Fig. 2, the differences are almost negative before the state returns to stable state, where high QoS should be adopted. In addition,

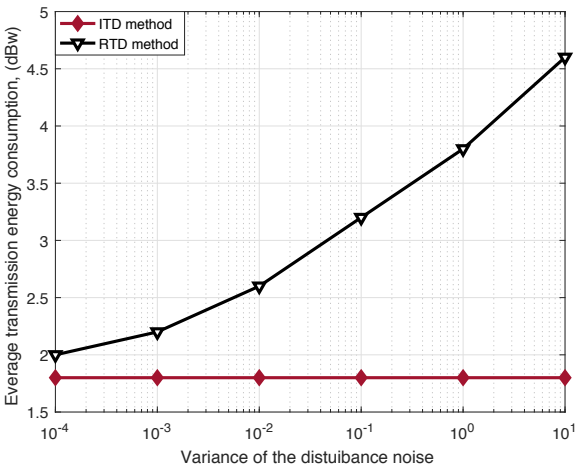

Fig. 7. Average transmission energy consumption with different disturbance noise.

the difference is larger than that in Fig. 2. This is reasonable since large sample period leads to large state change according to (3). The comparison between Fig. 2 and Fig. 3 provides the explanation for the control cost performance in the following Fig. 4.

Fig. 4 demonstrates the control cost of the proposed method in Section IV. From the figure, all the curves have an "U" shape. This is related to both the time delay of the wireless communications and the sample period of the control system. From the communication aspect, a large ratio of the time delay to sample period, i.e., d_k/h_k, leads to large control cost. Thus, when sample period is small, time delay is dominant in control cost. In addition, the control cost reduces with the sample period increasing, since it leads to small d_k/h_k. From the control aspect, a large sample period leads to large control cost [15]. Thus, affected by the two aspects, the curves have an "U" shape.

About the difference between the proposed method and single QoS service in Fig. 4, we can obtain that the control cost curves of the proposed method are lower than the conventional method only using high URLLC QoS when sample period is less than 400 ms, i.e., $100 \leq h_k < 400$. On the contrary, when $h_k \geq 400$, the control costs of the proposed method are almost the same as that served by only high communication QoS. This can be explained by the following two aspects. On the one hand, the advantage of the low QoS in the proposed method decreases with the sample period increasing since the control cost is determined by communications when the sample period is small. This is shown in Fig. 2, where the advantage of the low QoS service is significant when the index of the control process is larger than 5 and less than 13, i.e., $5 \leq k < 13$. This leads to that the proposed method is better than the conventional high QoS service. On the other hand, when the sample period is large, control cost is gradually determined by the control coefficient, i.e., the sample period, which offsets the advantage of the low QoS service in the proposed method. This can be seen from Fig. 2, where only high QoS service is adopted before the stable state when $h_k \geq 400$. In summary, the control cost of the proposed method is close to that only using high QoS, and the optimal control cost is about 500 when the control sample period is 400 ms.

About the difference between the two methods of proposed method in Fig. 4, we can obtain that the control cost of the ITD method in Algorithm 1 is a little less than that of the RTD method in Algorithm 2 when sample period is small, and then they gradually overlap. This is reasonable since the obtained threshold k_{th} in ITD method is more accuracy than that in RTD method, and the effect is large when the sample period is small, i.e., $100 \leq h_k \leq 400$. Furthermore, from Fig. 4, the optimal control cost when the sample period is $h_k = 400$ ms in RTD method is almost the same as that in ITD method, which indicates that the RTD method works well when disturbance noise is small.

2) Energy Consumption: Fig. 5 shows the wireless energy consumption of the proposed method. From the figure, all the curves decrease monotonously. This is reasonable since the control process is performed with the same time for different sample periods. Thus, large sample period leads to small sample points, which leads to small energy consumption. Compared with the energy consumption of only using low QoS, the energy consumption of our proposed method only increases about 5%. However, compared with high QoS, the proposed method reduces the energy consumption by about 80%. This is reasonable since the designed threshold significantly reduces the usage of high QoS in the control process. In summary, the energy consumption of the proposed method is significantly reduced compared with the conventional method only using high QoS.

About the difference between the two methods of proposed method in Fig. 5, we can obtain that the energy consumption of the ITD method is a little less than that of the RTD method when sample period is small, and then they gradually overlap. The reason is the same as that in Fig. 4.

B. Performance with Different Disturbance Noise

In this subsection, we consider the communication and control performance when the disturbance noise is different. From the above subsection, the adopted sample period is $h_k = 400$ ms.

1) Control Performance: Fig. 6 demonstrates the control cost of the proposed method when disturbance noise is different. From the figure, the curve of the ITD method is approximatively horizontal when disturbance noise is different. This is reasonable since the effect of disturbance noise is taken into account in ITD method. However, the curve of the RTD method increases monotonously with disturbance noise. This is reasonable since the larger disturbance noise leads to larger error in the obtained threshold k_{th}.

2) Energy Consumption: Fig. 7 shows the wireless energy consumption of the proposed method when disturbance noise is different. From the figure, the curve of the ITD method is approximatively horizontal when disturbance noise is different. However, the curve of the RTD method increases monotonously with disturbance noise. The reasons for the above two phenomena are the same as that in Fig. 6.

3) Summary: From Fig. 6 and 7, the disturbance noise have large effect on both the control performance and communication performance. The control cost and communication energy consumption of the RTD method increase monotonously with the disturbance noise. In addition, the simulation results indicate that the RTD method works well when the disturbance noise is small.

VI. Conclusions and Future Works

In this paper, we proposed a dynamic communication QoS allocation method throughout the control process to reduce the communication energy consumption, which is based on communication-control co-design. In our method, we answered an important question when high URLLC QoS is critical for the control performance and when the QoS can be relaxed to a lower level. Then, we proposed an ITD method and a RTD method considering the actual scenarios to obtain the threshold for the dynamic QoS selection. Furthermore, we analyzed the feasibility of the dynamic QoS selection, where both the effect of the communication time delay and reliability on the control performance were provided. From the analysis, we obtained that low communication QoS can provide better control performance than high QoS at certain stage in the control process. Simulation results showed the proposed method can significantly reduce the communication energy consumption while maintaining similar control performance only using high QoS. With our method, the real-time control systems can be performed more efficiently using significantly less wireless resource in wireless communications.

However, as one of the first trails discussing the effect of the dynamic wireless communication design on the control performance by communication-control co-design, there are many other problems should be to dealt with. For instance, a more effective method is desired to determine the threshold in different disturbance noise cases. In addition, the scenario that both the uplink and downlink experience time delay and packet loss should be discussed. Furthermore, the validation in this paper is only done by simulation, where the experiments on the platform is needed to evaluate the performance of the proposed method. In our future work, we would first propose some platform schemes, and then assess them by analyzing large amounts of wireless data collected from different industrial environments according to [35]. After the assessment, we choose the best scheme to evaluate the performance of the proposed method on the platform. This would provide solid validation of the whole system.

Appendix A

This appendix provides the detailed calculation of the parameters in (8) and (9).

According to [15], $\mathbf{S}_k$ is calculated by

$$\begin{aligned}\mathbf{S}_k =&\boldsymbol{\Omega}_d^T\mathbf{S}_{k+1}\boldsymbol{\Omega}_d + \mathbf{W} - \boldsymbol{\Omega}_d^T\mathbf{S}_{k+1}\boldsymbol{\Phi}_d(\boldsymbol{\Phi}_d^T\mathbf{S}_{k+1}\boldsymbol{\Phi}_d \\ &+ U)^{-1}\boldsymbol{\Phi}_d^T\mathbf{S}_{k+1}\boldsymbol{\Omega}_d,\end{aligned} \tag{25}$$

The generalized state can be estimated by a modified Kalman filter, which can be obtained as follows.

- Step 1: prior generalized state estimation. The prior estimation for the generalized state can be expressed as

$$\hat{\xi}_{k+1|k} = \boldsymbol{\Omega}_d\hat{\xi}_{k|k} + \boldsymbol{\Phi}_d u_k, \tag{26}$$

  where $\hat{\xi}_{k|k}$ is the generalized state estimation based on the current generalized state, and $\hat{\xi}_{k+1|k}$ is the generalized state estimation at time $k+1$ based on the last generalized state at k.
- Step 2: prior error variance estimation. The prior estimation for the error variance can be expressed as

$$\mathbf{P}_{k+1|k} = \boldsymbol{\Omega}_d\mathbf{P}_{k|k}\boldsymbol{\Omega}_d^T + \mathbf{R}_n, \tag{27}$$

  where $\mathbf{P}_{k|k} = \mathbb{E}[(\xi_k - \hat{\xi}_k)(\xi_k - \hat{\xi}_k)^T]$ is the estimation error variance, and $\mathbf{P}_{k+1|k}$ is the prior estimation error variance at time $k+1$.
- Step 3: optimal generalized state estimation. The optimal generalized state estimation is the generalized state estimation based on $\hat{\xi}_{k+1|k}$, and can be expressed as

$$\hat{\xi}_{k+1|k+1} = \hat{\xi}_{k+1|k} + l_k\mathbf{K}_{k+1}(\mathbf{y}_{k+1} - \mathbf{C}_d\hat{\xi}_{k+1|k}), \tag{28}$$

  where $\mathbf{K}_{k+1}$ will be discussed in the following Step 4.
- Step 4: optimal control gain estimation. The optimal control gain estimation $\mathbf{K}_{k+1}$ can be expressed as

$$\mathbf{K}_{k+1} = \mathbf{P}_{k+1|k}\mathbf{C}_d^T(\mathbf{C}_d\mathbf{P}_{k+1|k}\mathbf{C}_d^T + R_{n'})^{-1}. \tag{29}$$

- Step 5: optimal error variance estimation. The optimal error variance estimation is the error variance estimation based on $\mathbf{P}_{k+1|k}$, which can be calculated by

$$\mathbf{P}_{k+1|k+1} = \mathbf{P}_{k+1|k} - l_k\mathbf{K}_{k+1}\mathbf{C}_d\mathbf{P}_{k+1|k}. \tag{30}$$

Finally, substituting the above parameters into (8), we can obtain (9). Furthermore, to minimize the control cost in (8), the control input needs to satisfy the following expression

$$\begin{aligned}u_k &= -\left(\boldsymbol{\Phi}_d^T\mathbf{S}_{k+1}\boldsymbol{\Phi}_d + \mathbf{U}\right)^{-1}\boldsymbol{\Phi}_d^T\mathbf{S}_{k+1}\boldsymbol{\Omega}_d\hat{\xi}_{k|k} \\ &= -\mathbf{L}_k\hat{\xi}_{k|k}.\end{aligned} \tag{31}$$

References

[1] M. Simsek, A. Aijaz, M. Dohler, J. Sachs, and G. Fettweis, "The 5G-enabled tactile internet: applications, requirements, and architecture," *IEEE Wireless Commun. and Networking Conf.*, Apr. 2016, pp. 1-6.

[2] M. Simsek, A. Aijaz, M. Dohler, J. Sachs, and G. Fettweis, "5G-enabled tactile internet," *IEEE J. Selected Areas Commun.*, vol. 34, no. 3, pp. 460-473, Feb. 2016.

[3] 3GPP, *Study on Scenarios and Requirements for Next Generation Access Technologies*. Technical Specification Group Radio Access Network, Technical Report 38.913, Release 14, Oct. 2016.

[4] M. Simsek, A. Aijaz, M. Dohler, J. Sachs, and G. Fettweis, "5G-enabled tactile internet," *IEEE J. Select. Areas Commun.*, vol. 34, no. 3, pp. 460-473, Mar. 2016.

[5] B. Chang, G. Zhao, Z. Chen, L. Li, and M. A. Imran, "Packet-drop design in URLLC for real-time wireless control systems," *IEEE ACCESS*, vol. PP, no. PP, pp. 1-10, Jul. 2019.

[6] B. Chang, L. Zhang, L. Li, G. Zhao, and Z. Chen, "Optimizing resource allocation in URLLC for real-time wireless control systems," *IEEE Trans. Veh. Tech.*, vol. PP, no. PP, pp. 1-13, Jul. 2019.

[7] S. Mumtaz, A. Alsohaily, Z. Pang, A. Rayes, K. Tsang, and J. Rodriguez, "Massive internet of things for industrial applications: addressing wireless IIoT connectivity challenges and ecosystem fragmentation," *IEEE Industrial Electronics Mag.*, vol. 11, no. 1, pp. 28-33, Mar. 2017.

[8] C. Sun, C. She, and C. Yang, "Energy-efficient resource allocation for ultra-reliable and low-latency communications," *IEEE Globecom*, Dec. 2017, pp. 1-6.

[9] C. Sun, C. She, and C. Yang, "Exploiting multi-user diversity for ultra-reliable and low-latency communications," *IEEE Globecom Workshops (GC Wkshps)*, Dec. 2017, pp. 1-6.

[10] C. She, Ch. Yang, and T. Q. S. Quek, "Uplink transmission design with massive machine type devices in tactile internet," *IEEE Globecom Workshops (GC Wkshps)*, Dec. 2016, pp. 1-6.

[11] C. She, C. Yang, and T. Quek, "Cross-layer optimization for ultra-reliable and low-latency radio access networks," *IEEE Trans. Wireless Commun.*, vol. PP, no. 99, pp. 1-15, Oct. 2017.

[12] B. Singh, O. Tirkkonen, Z. Li, and Mikko A. Uusitalo, "Contention-based access for ultra-reliable low latency uplink transmissions," *IEEE Wireless Commun. Lett.*, vol. PP, no. 99, pp. 1-4, Oct. 2017.

[13] J. Nielsen, R. Liu, and P. Popovski, "Ultra-reliable low latency communication (URLLC) using interface diversity," *IEEE Trans. Commun.*, vol. 66, no. 3, pp. 1322-1334, Mar. 2018.

[14] C. She, C. Yang, and T. Quek, "Radio resource management for ultra-reliable and low-latency communications," *IEEE Commun. Mag.*, vol. 55, no. 6, pp. 72-78, Jun. 2017.

[15] L. Schenato, B. Sinopoli, M. Franceschetti, K. Poola, and S. Sastry, "Foundations of control and estimation over lossy networks," *IEEE Proc.*, vol. 95, no. 1, pp. 163-187, Jan. 2007.

[16] P. Park, S. Ergen, C. Fischione, C. Lu, and K. Johansson, "Wireless network design for control systems: a survey," *IEEE Commun. Surveys Tutorials*, vol. PP, no. 99, pp. 1-36, Dec. 2017.

[17] X. Ge and Q. Han, "Distributed formation control of networked multi-agent systems using a dynamic event-triggered communication mechanism", *IEEE Trans. Industrial Electronics*, vol. 64, no. 10, pp. 8118-8127, Oct. 2017.

[18] M. Luvisotto, Z. Pang, and D. Dzung, "Ultra high performance wireless control for critical applications: challenges and directions," *IEEE Trans. Industrial Informatics*, vol. 13, no. 3, pp. 1448-1459, Jun. 2017.

[19] Y. Chen, L. Cheng, and L. Wang, "Prioritized resource reservation for reducing random access delay in 5G URLLC," *IEEE Annual Inter. Symposium Personal, Indoor, and Mobile Radio Communications (PIMRC)*, Oct. 2017, pp. 1-5.

[20] B. Chang, G. Zhao, M. Imran, L. Li, and Z. Chen, "Dynamic QoS allocation for real-time wireless control in tactile internet," *IEEE 5G World Forum (WF5G)*, Jul. 2018, pp. 1-5.

[21] B. Chang, G. Zhao, M. Imran, Z. Chen, and L. Li, "Dynamic wireless QoS analysis for real-time control in URLLC," *IEEE Globecom Workshops (GC Wkshps)*, Dec. 2018, pp. 1-4.

[22] 3GPP Mobile Broadband Innovation Path to 4G, "Release 9, Release 10 and Beyond, HSPA+ LTE/SEA and LTE-Advanced," 3GAmericas, Feb.2010.

[23] P. Park, J. Araújo, and K. H. Johansson, "Wireless networked control system co-design," *IEEE Inter. Conf. Networking, Sensing and Control (ICNSC)*, 2011, pp. 486-491.

[24] S. Cai and V. Lau, "Zero MAC latency sensor networking for cyber-physical systems," *IEEE Trans. Signal Processing*, vol. 66, no. 14, pp. 3814-3823, Jul. 2018.

[25] O. Boubaker and R. Iriarte, *The inverted pendulum in control theory and robotics: from theory to new innovations*, Institution of Engineering and Technology, Dec. 2017.

[26] M. Luvisotto, Z. Pang, and D. Dzung, "High-performance wireless networks for industrial control applications: new targets and feasibility," *Proceedings of the IEEE*, vol. 107, no. 6, pp. 1074-1093, Jun. 2019.

[27] J. Nilsson, *Real-time control systems with delays*, Ph.D. dissertation, Sweden, Jan. 1998.

[28] F. Rasool and S. Nguang, "Networked control systems," *Lecture Notes in Control and Information Sciences*, vol. 52, no. 9, pp. 318-323, Sep. 2008.

[29] *Physical Layer Aspects for Evolved Universal Terrestrial Radio Access (UTRA)*, 3GPP TR 25.814, 2006.

[30] W. Yang, G. Durisi, T. Koch, and Y. Polyanskiy, "Quasi-static multiple-antenna fading channels at finite blocklength," *IEEE Trans. Inf. Theory*, vol. 60, no. 7, pp. 4232-4264, Jul. 2014.

[31] G. Durisi, T. Koch, and P. Popovski, "Toward massive, ultrareliable, and low-latency wireless communication with short packets," *Proc. IEEE*, vol. 104, no. 9, pp. 1711-1726, Sep. 2016.

[32] K. Gatsis, M. Pajic, A. Ribeiro, and G. J. Pappas, "Opportunistic control over shared wireless channels," *IEEE Trans. Automatic Control*, vol. 60, no. 12, pp. 3140-3155, Dec. 2015.

[33] E. Chong and S. Żak, An Introduction to Optimization (4th Edition), New York: Wiley, 2001.

[34] S.Boyd and L. Vandenberghe, *Convex Optimization*, Cambridge University Press, 2004.

[35] X. Jiang, Z. Pang, M. Luvisotto, F. Pan, R. Candell, and C. Fischione, "Using large data Set to improve wireless communications: latency, reliability, and security," *IEEE Industrial Electronics Mag.*, vol. 13, no. 1, pp. 6-12, Mar. 2019.